DOI: 10.1002/ejic.200801032

Assembly of Novel 2D and 3D Heterometallic Sb^{III}–Cu^{I} Polymers Based on Antimony(III) Thiolates as Metallothiolato Ligands

Zhi-Hua Li,[a] Long-Hua Li,[a] Li-Ming Wu,[a] and Shao-Wu Du*[a]

Dedicated to Professor Xin-Tao Wu on the occasion of his 70th birthday

Keywords: Coordination polymers / Antimony / Structure elucidation / Band gap / Density functional calculations

A new type of neutral heterometallic Sb^{III}–Cu^{I} thiolate coordination polymer has been synthesized under solvothermal conditions by using antimony(III) thiolates as metalloligands and CuSCN as the source of the second metal ion. Reaction of [Sb(edt)Cl] (**1**) (edt = ethane-1,2-dithiolate) with 1 equivalent of CuSCN affords $[\{Sb_2(edt)_2(\mu_3\text{-}S)CuCl(CuSCN)\}_n]$ (**2**), which features a 2D layer consisted of –CuSCNCuSCN– chains and $\{Sb_2(edt)_2(\mu_3\text{-}S)CuCl\}$ units. During the reaction, **1** was converted into a sulfur-bridged dimer $Sb(edt)_2S$, which behaves simultaneously as a bridging and chelating ligand through all of its sulfur atoms to connect four Cu^+ ions in the framework structure of **2**. Replacement of Cl^- in **1** with $pymt^-$ gives a new antimony(III) thiolate formulated as [Sb(edt)(pymt)] (**3**) (pymt = 2-pyrimidinethiol), which was further treated with CuSCN to afford coordination polymers $[\{[Sb(edt)(pymt)]_2(CuSCN)_3\}_n]$ (**4**) and $[\{[Sb(edt)(pymt)](CuSCN)_2\}_n]$ (**5**). In the assemblies of **4** and **5**, the structure of **3** remains intact and the whole compound serves as a multidentate ligand through S_{edt} and N_{pymt} atoms to Cu^+ ions. Complex **4** also contains –CuSCNCuSCN– chains, which are linked by tridentate {Sb(edt)(pymt)} fragments to form a 2D polymer. Complex **5** is a 3D architecture with {Sb(edt)(pymt)} units acting as bidentate bridging ligand to link the $(CuSCN)_n$ layers and $\{(CuSCN)_2\}_n$ columns. Complexes **2**–**5** showed optical transitions with band gaps of 2.66 to 3.41 eV, and their optical properties were studied by DFT calculations.

Introduction

The chemistry of heterometallic thiolate complexes has been an active area of research because of their relevance to biological systems, their great structural diversity, and practical or potential applications for fuel cells, nonlinear optical materials, semiconductors, and electrochemical sensors.[1–3] Many transition-metal thiolates $M(SR)_n$ (M = Cu, Ag, Zn, Cd, Fe, etc.; n = 1–4) have been utilized as versatile building blocks to combine with other metal ions in the preparation of mixed-metal thiolate complexes or coordination polymers.[2,4] Although a number of main-group metal thiolates with monomeric to polymeric structures have been synthesized and structurally characterized since 1948,[5–11] they have seldom been used as building blocks for the assembly of heterometallic thiolates. Recent examples include the ternary molecular cluster anion $[Bi_{10}Cu_{10}(SPh)_{24}]^{2-}$ and the cluster cation $[Sn_3Cu_4(edt)_6(\mu_3\text{-}O)(PPh_3)_4]^{2+}$ (edt = ethane-1,2-dithiolate).[2b,2c] For antimony thiolates with transition metals, a database search reveals only two compounds $[Pt(PPh_3)_2\{Sb(SPh)_3\}_2]$ and $[(CO)_5W(\mu\text{-}StBu)Sb(StBu)_2]$.[11] These complexes produced to date are limited to discrete molecules and the coordination polymers with main-group elements and transition metals bridged by thiolato ligands have not been seen, although the open-framework materials, in which transition-metal cations (TM^{n+}) are incorporated within the main-group-sulfide frameworks, have been the subject of recent investigations because of their novel structures and semiconducting properties.[12–14]

An obvious approach to heterometallic thiolates containing both main-group elements and transition metals would involve the use of main-group thiolates as metalloligands. This methodology is best demonstrated by the synthesis of the above-mentioned mixed-metal cluster cation $[Sn_3Cu_4(edt)_6(\mu_3\text{-}O)(PPh_3)_4]^{2+}$, in which the precursor complex $[Sn(edt)_2]$ was deployed as a ligand for Cu atoms.[2b] In this present study, the antimony(III) thiolates [Sb(edt)Cl] (**1**) and [Sb(edt)(pymt)] (**3**) (pymt = 2-pyrimidinethiol) were chosen as metalloligands because they offer thiol and pyridyl functionalities available for bonding to other metal ions. Such complexes can themselves be considered as new

[a] State Key Laboratory of Structural Chemistry, Fujian Institute of Research on the Structure of Matter, Chinese Academy of Sciences,
Fujian, Fuzhou 350002, P. R. China
Fax: +86-591-83709470
E-mail: swdu@fjirsm.ac.cn

Supporting information for this article is available on the WWW under http://www.eurjic.org/ or from the author.

metal-containing ligands and subsequently allowed to self-assemble with other metal ions through the free donor sites. Furthermore, the rigid and stereo molecular geometry of **1** and **3** relative to free edt^{2-} or $pymt^{-}$ was expected to induce the formation of multidimensional patterns in the aggregation of the complexes in the solid state. Accordingly, the solvothermal reactions of **1** and **3** with CuSCN gave three new coordination polymers, namely, $[\{Sb_2(edt)_2(\mu_3\text{-}S)CuCl(CuSCN)\}_n]$ (**2**), $[\{[Sb(edt)(pymt)]_2(CuSCN)_3\}_n]$ (**4**), and $[\{[Sb(edt)(pymt)](CuSCN)_2\}_n]$ (**5**), which are the first examples of heterometallic coordination polymers containing both antimony thiolates and copper metal centers.

Results and Discussion

Synthesis

As shown in Scheme 1, when [Sb(edt)Cl] (**1**) was heated with 1 equivalent of CuSCN in acetone at 120 °C for 48 h, pale yellow crystals of $[\{Sb_2(edt)_2(\mu_3\text{-}S)CuCl(CuSCN)\}_n]$ (**2**) were isolated in low yield. The mechanism for the formation of the sulfur-bridged dimer $\{Sb_2(edt)_2S\}$ in **2** is obscure. We speculate that the cleavage of the Sb–Cl bonds occurred during the reaction and the resulting $\{Sb(edt)\}^+$ moieties deprived of sulfur atoms, probably from SCN^- groups to form $\{Sb_2(edt)_2S\}$, which then linked Cu ions to afford 2D layers. This desulfuration of SCN^- groups under solvothermal conditions was observed in other reaction systems.[15] This in situ formation of $\{Sb_2(edt)_2S\}$ may be responsible for the low yield of **2**. Adding inorganic sulphide in an attempt to improve the yield of **2** gave a large amount of white deposition but no crystals of **2**. Treatment of **1** with pymtNa in ethanol generated the desired [Sb(edt)(pymt)] (**3**) in moderate yield. The XRD patterns showed that the product **3** prepared by this method is pure (Figure S1). This species contains two different thiolato ligands edt and pymt and can be used as a mixed-thiolato metalloligand for the further reactions. The reaction of **3** with 1.5 equivalents of CuSCN at 120 °C in CH_3CN afforded yellow block crystals of $[\{[Sb(edt)(pymt)]_2(CuSCN)_3\}_n]$ (**4**). The use of 2 equiv. CuSCN in a similar reaction resulted in the formation of a mixture of **4** and a small amount of orange-red crystals of $[\{[Sb(edt)(pymt)](CuSCN)_2\}_n]$ (**5**). Crystals of **4** and **5** were separated manually. Attempts to increase the yield of **5** by changing the reaction conditions, for example, by using more CuSCN, increasing the reaction temperature, or using **4** as the starting reactant, failed. In the formation of polymers **4** and **5**, the structure of **3** remains unchanged, and **3** functions as neutral tri- and didentate metalloligands, respectively, to bind with the Cu atoms. This situation is in contrast to the formation of **2**, in which [Sb(edt)Cl] was converted into a new antimony(III) thiolate $\{Sb_2(edt)_2S\}$ with transfer chloride to Cu^+ ion in the final product, presumably as a result of differences in the stabilities of **3** and **1** under the solvothermal conditions. The choice of appropriate copper salts is essential to this reaction system. So far, we have only succeeded in the preparation of Sb^{III}–Cu^{I} polymers by using CuSCN. Similar reactions of **3** with other different copper sources, such as CuCN and CuI, under the same conditions have also been performed in attempts to prepare analogous complexes. However, these reactions led to isolation of intractable materials and none of the desirable compounds was formed. Complexes **2**–**5** are air stable and have been characterized by spectroscopic methods.

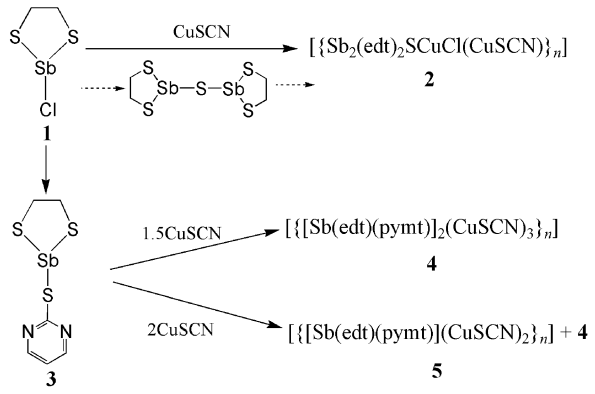

Scheme 1. The synthesis of compounds **2**–**5**.

Crystal Structure of 2

The crystal structure of **2** features a 2D layer constructed from –CuSCNCuSCN– chains, CuCl, and $\{Sb_2(edt)_2S\}$ units (Figure 1). The Sb1 center is ligated by two S_{edt} atoms [*d*(Sb1–S2) = 2.465(2) Å; *d*(Sb1–S3) = 2.484(2) Å] and one inorganic sulfur atom [*d*(Sb1–S1) = 2.457(1) Å]. The coordination environment around the Sb atom would be best described as trigonal pyramidal with the lone pair of electrons in the axial position *trans* to the Sb–S bonds, but with nonequivalent S–Sb–S bond angles [96.30(5), 86.70(6), and 87.27(4)°]. The short distances of Sb1···S4 [3.662(2) Å], Sb1···S2C [3.864(2) Å], and Sb1···Cl1E [3.023(2) Å] indicate the existence of secondary interactions.[7e] The inorganic S1 atom bridges two $\{Sb(edt)\}^+$ cations to form the dimer $\{Sb_2(edt)_2S\}$. As shown in Scheme 2(a), the entire $\{Sb_2(edt)_2S\}$ unit serves as multidentate thio ligands to link four Cu^+ ions through the Cu–S bonds. Both Cu1 and Cu2 are

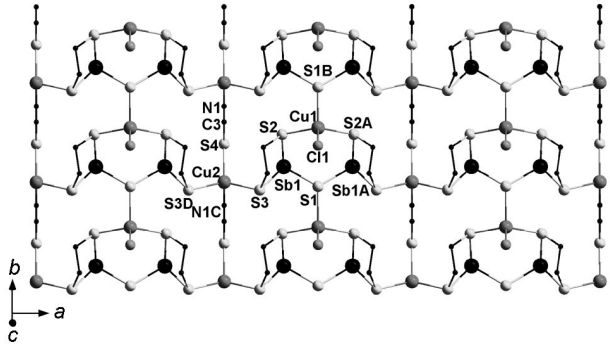

Figure 1. Perspective view of part of the layer in complex **2** with atom numbering scheme. All hydrogen atoms are omitted for clarity. Symmetry code: A: 1 – *x*, *y*, *z*; B: *x*, 1 + *y*, *z*; C: *x*, –1 + *y*, *z*; D: –*x*, *y*, *z*.

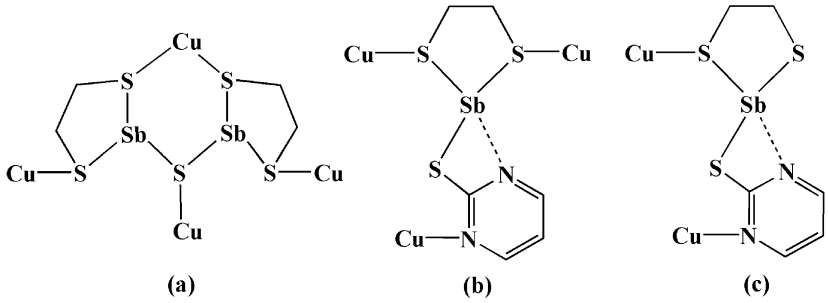

Scheme 2. The coordination mode of $\{Sb_2(edt)_2S\}$ in **2** (a) and the coordination modes of metalloligand **3** in **4** (b) and **5** (c).

tetrahedrally coordinated but in different environments. The Cu1 atom coordinates to two S atoms from different Sb-chelating edt ligands in the same $\{Sb_2(edt)_2S\}$ unit, one inorganic S atom from another $\{Sb_2(edt)_2S\}$ unit, and one Cl atom, whereas Cu2 coordinates to two S_{edt} atoms from the neighboring $\{Sb_2(edt)_2S\}$ units, one S atom, and one N atom from different SCN^- ligands. In this way, each Cu2 atom links two SCN^- ligands to form a –CuSCNCuSCN– linear chain along the *b* axis, and each Cu1 atom connects two $\{Sb_2(edt)_2S\}$ units to form a $\{Sb_2(edt)_2S\}$CuCl chain along the same direction. These two kinds of distinct chains are joined together by the Cu–S contacts and arranged in alternate positions throughout the *ab* plane to produce a neutral 2D layer (Figure 1). The distances between the adjacent layers are around 5.7 Å (Figure S2). If the secondary Sb···Cl interactions are taken into account, the 2D layers in **2** can be further linked into a 3D network (Figure S2).

Crystal Structure of 3

Complex **3** crystallizes in the space group *C*2/*c* and consists of one Sb atom, one edt, and one pymt ligand in its asymmetric unit (Figure 2). The Sb1 atom is four-coordinate and its coordination geometry is distorted from regular trigonal pyramidal by the influence of the Sb–N secondary interaction. The Sb1–S_{edt} distances [*d*(Sb1–S1) = 2.431(2) Å and *d*(Sb1–S2) = 2.457(1) Å] are slightly longer than those in [Sb(edt)Cl] [2.401(4) and 2.412(5) Å] probably because of the bulky steric effect of the pymt ligand compared with that of the Cl^- ion. The Sb1–S_{pymt} distance of 2.5135(9) Å is slightly longer than those of Sb1–S1 and Sb1–S2 and that observed for $[Sb(2\text{-}SC_5H_4N)_3]$ [2.470(1) Å], but is close to those found for $[Sb(2\text{-}SC_5H_4N\text{-}3\text{-}SiMe_3)_3]$ [2.509(2) and 2.520(2) Å].[7d] The Sb1–N1 distance of 2.853(4) Å, which is in agreement with that of $[Sb(2\text{-}SC_5H_4N)_3]$, is significantly longer than the anticipated single-bond length of 2.50–2.65 Å but is still shorter than the sum of the van der Waals radii of Sb and N.[7d] As observed previously, such long or secondary bonding is a common characteristic of the structural behavior of main-group metals particularly those containing stereochemically active lone pairs. The geometric consequence of the Sb1–N1 secondary bonding is that the S2–Sb1–S3 angle of 97.61(4)° is more expanded than those of S1–Sb1–S2 and S1–Sb1–S3 [87.40(3)° and 91.09(4)°]. In **3**, one of the N atoms of the Sb-chelating pymt ligand remains uncoordinated; therefore, it can be used as a multidentate metalloligand through both its N and S donors.

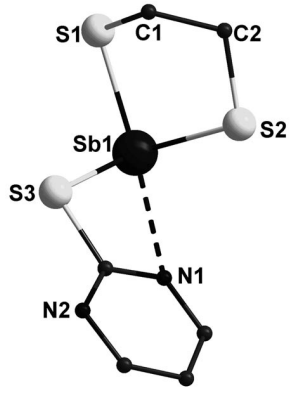

Figure 2. Asymmetric unit in **3** with atom numbering scheme. All hydrogen atoms are omitted for clarity.

Crystal Structure of 4

Complex **4** is characterized by a 2D layer constructed from –CuSCNCuSCN– chains and tricoordinated {Sb(edt)(pymt)} building blocks (Figure 3). There are two {Sb(edt)(pymt)} and three CuSCN units in its asymmetric unit. The {Sb(edt)(pymt)} unit functions as a metalloligand to link three Cu atoms by its two S_{edt} atoms and one uncoordinated N atom from a pymt ligand [Scheme 2(b)]. The dimensions of this unit are virtually identical to that of **3**, except for some variations in the Sb–S bond lengths. In comparison to those in **3**, the Sb–S_{edt} distances ranging from 2.4681(8) to 2.4931(7) Å are slightly elongated, whereas the Sb–S_{pymt} distances of 2.4681(8) and 2.4728(8) Å are somewhat shortened. The elongation of Sb–S_{edt} is due to the additional coordination of the edt ligand to the Cu atoms and is in accordance with an observation reported for $[Sn_3Cu_4(edt)_6(\mu_3\text{-}O)(PPh_3)_4]^{2+}$.[2b] All the Cu^I atoms are four-coordinate with two S atoms from the adjacent edt ligands and one S atom and one N atom from the SCN^- ions. The Cu atoms are bridged by the SCN^- groups to form a –CuSCNCuSCN– single chain along the *c* axis;

these chains are linked by the Sb(edt)(pymt) units to give a 2D layer extended in the *bc* plane (Figure 3). These 2D layers are parallel to each other as shown in Figure S3, and the distances between the adjacent layers are about 7.0 Å.

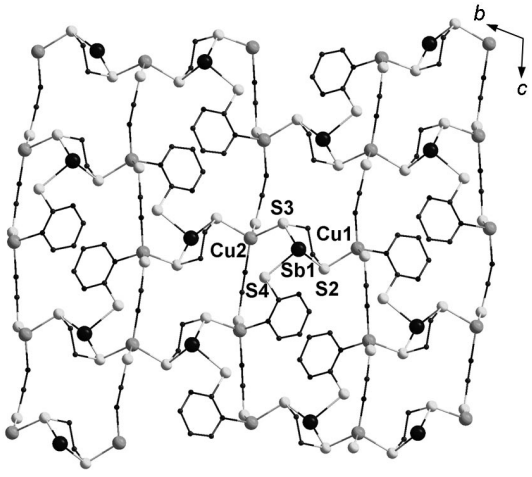

Figure 3. Perspective view of part of the layer in **4**. All hydrogen atoms are omitted for clarity.

Crystal Structure of 5

Compared with compound **4**, which contains CuSCN and {Sb(edt)(pymt)} units in a ratio of 3:2, there are two CuSCN and one {Sb(edt)(pymt)} unit in the asymmetric unit of **5**. Compound **5** features a 3D network constructed from 2D (6,3) layers $(CuSCN)_n$, 1D $\{(CuSCN)_2\}_n$ columns, and {Sb(edt)(pymt)} units (Figure 4). Similar to **4**, the {Sb(edt)(pymt)} unit in **5** also acts as a metalloligand to bind with Cu atoms but in a slightly different way in that only one S_{edt} atom was involved in the coordination to the Cu atom [Scheme 2(c), Figure 4(a)]. The Sb–S distances in **5** ranging from 2.429(2) to 2.500(2) Å are comparable to those in **3** and **4**, whereas the Sb1–N3 distance of 2.647(5) Å is significantly shorter than those in **3** or **4** and close to that of a Sb–N single bond.[16] The Cu1 adopts a distorted tetrahedral geometry, coordinating to one N atom and two S atoms from three μ_3-SCN^- groups and one N atom from a pymt ligand. The $\{(CuSCN)_2\}_n$ column containing Cu1 can be described as two zigzag chains arranged with approximate C_{2v} symmetry, one chain being connected to the other by the Cu–S contacts [Figure 4(b)]. The distance of Cu1···Cu1a is 2.867(2) Å, indicating the existence of weak metal interactions. Although many kinds of $\{(CuSCN)_2\}_n$ columns have been reported for related copper thiocyanate compounds with N-donor ligands, as best as we know, only one example with this kind of structure has been reported recently.[17] The Cu2 atom within a 2D $(CuSCN)_n$ layer also adopts a distorted tetrahedral geometry, which is coordinated by two S atoms and one N atom from three μ_3-SCN^- groups and one S atom from an edt ligand. As shown in Figure 4(b), each of the ten-membered (Cu–S–Cu–NCS–Cu–SCN) rings is fused with six other rings to give a distorted honeycomb pattern, which can be also regarded as a (6,3) net from a topological perspective. The {Sb(edt)(pymt)} metalloligands connect the Cu atoms of a 2D $(CuSCN)_n$ layer on one side through S_{edt} atoms

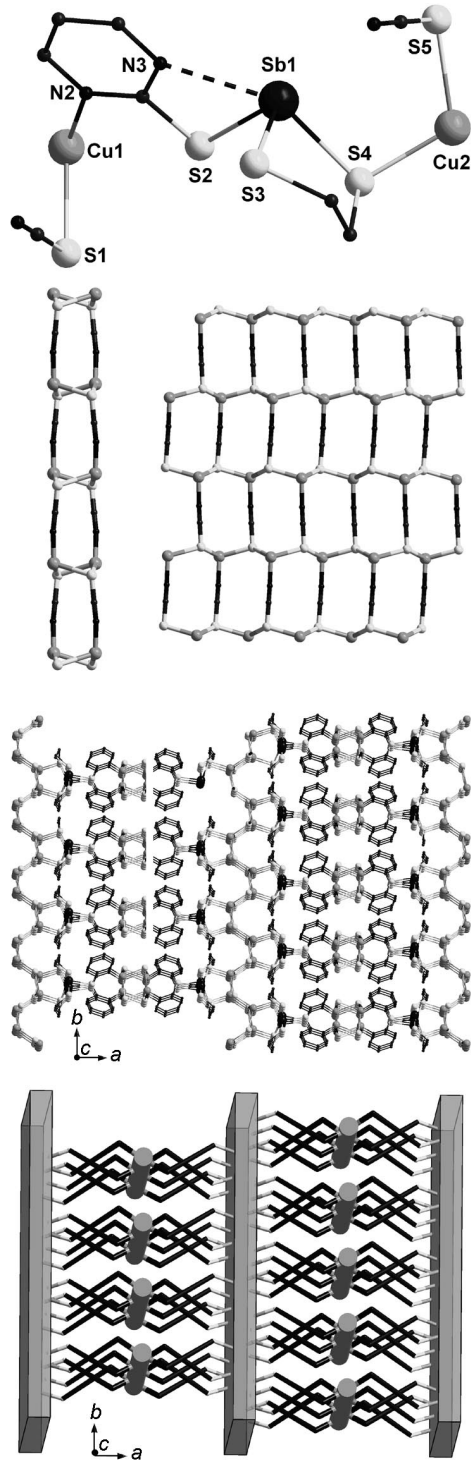

Figure 4. (a) The coordination mode of metalloligand **3** in **5**. (b) View of the $\{(CuSCN)_2\}_n$ column (left) and the (6,3) layer of $\{CuSCN\}_n$ (right) in **5**. (c) Part of the 3D structure and (d) its schematic representation constructed from $\{(CuSCN)_2\}_n$ columns and $\{CuSCN\}_n$ layers in **5**. All hydrogen atoms are omitted for clarity.

and the Cu atoms of a stack of $\{(CuSCN)_2\}_n$ columns through N_{pymt} atoms on the other side, thus creating a 3D framework [Figure 4(c)]. To the best of our knowledge, **5** is the first example of 3D coordination polymer with two distinct motifs of copper(I) thiocyanate coexisting in the crystal structure.

Infrared Spectra

The strong bands observed in the spectra of **2**, **4**, and **5** at 2078, 2100, and 2126 cm^{-1}, respectively, are assigned to the $\nu_{C\equiv N}$ vibration from the SCN^- groups. The C–S stretches at 669 and 636 cm^{-1} in **2** are comparable to those observed in **1** or [As(edt)Cl].[18] The infrared spectra of **3**–**5** show distinct vibrational bands in the regions around 1550 and 1370 cm^{-1}, which have been assigned as ν_{C-N} vibrations (thioamide I and II bands) and in the regions around 1180 and 809 cm^{-1}, which are attributed to C–S bond vibrations (thioamide III and IV bands). Relative to the corresponding thioamide bands of the free thione ligand (pymtH) at 1510, 1320, 982, and 793 cm^{-1}, bands I–IV in **3**–**5** are shifted to higher frequencies, indicating nitrogen and sulfur donation of the pymt ligand in bonding with the metal ions.[19] This shift of the infrared spectra of the pymt ligand has also been observed in the related compound $[Sb(pymt)_3]$.[7b]

Optical Absorption Spectra

The optical absorption spectra of **1**–**5** and CuSCN were measured by diffuse-reflectance experiments. The UV/Vis absorption data were calculated from the reflectance data by using the Kubelka–Munk function: $\alpha/S = (1 - R)^2/2R$,[20] where R is the experimentally observed reflectance, α the coefficient, and S the scattering coefficient. The spectra reveal the presence of the optical gaps, as shown in Figure 5. The band gaps of **1**–**5** and CuSCN were assessed to be approximately 3.28, 2.80, 3.41, 2.84, 2.66, and 3.72 eV, respectively, determined as the intersection point by $(\alpha/S)^2 = 0$ in a $(\alpha/S)^2$ versus E plot (Figure S4).[21] The band gaps of 2D to 3D compounds **2**, **4**, and **5** are significantly smaller than those of their discrete precursors **1** and **3**, and are much smaller than that of CuSCN. These results show that compounds **2**–**5** may be classed as semiconductors.

DFT calculations showed that the band gaps of **2**–**5** were 2.12, 2.25, 1.63, and 1.29 eV, respectively, which is about 24.3–51.5% less than that derived from the experimental results. This band-gap difference is an ordinary problem for the discussion of the spectra of solids using DFT eigenvalues.[22] As for the general gradient approximation (GGA), the predicted band gap is typically 30–50% smaller than those observed in experiments.

The bands can be assigned according to the total and partial densities of states (DOS) of **2**–**5**, as plotted in Figure 6. The total density of states at the top of the valance bands (VBs) in **2**, **4**, and **5** are almost formed by S 3p and Cu 3d states, whereas the top of the VBs of **3** is formed mostly by the S 3p state mixing with a small amount of the N 2p state. As shown in Figure 6(a), the bottom of the conduction bands (CBs) of **2** is almost a contribution from Sb 5p and S 3p states. Accordingly, the optical absorption of **2** can be ascribed as charge transitions from S 3p and Cu 3d states to Sb 5p and S 3p states. As for compounds **3**–**5** containing pyrimidines in their molecules, the bottom of CBs derives mostly from C 2p and N 2p states, and Sb or S creates almost no contribution. Therefore, the absorption peaks of **3**–**5** can be assigned as charge-transfer transitions from occupied S 3p and N 2p states (**3**) or S 3p and Cu 3d states (**4** and **5**) to empty C 2p and N 2p states. The DFT calculations indicated that the band gaps of **3**–**5** decrease with an increase of the dimension of their structures, $\Delta E_g(\mathbf{3}) > \Delta E_g(\mathbf{4}) > \Delta E_g(\mathbf{5})$, which is consistent with the experimental trend shown in Figure 5.

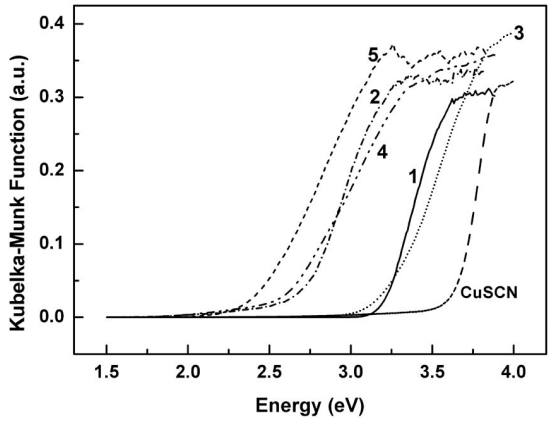

Figure 5. Room-temperature optical adsorption spectra for solid samples of **1**–**5** and CuSCN.

Conclusions

In summary, we have synthesized three heterometallic thiolate polymers **2**, **4**, and **5** under solvothermal conditions by using antimony(III) thiolates **1** and **3** as metalloligands. These complexes represent the first examples of coordination polymers containing both main-group elements and transition metals with thiolato ligands. The optical properties of compounds **2**–**4** have been studied by diffuse-reflectance experiments and the results reveal that they may be classed as semiconductors. In the formation of **2**, a new thiolantimonate $\{Sb_2(edt)_2S\}$ was formed, whereas in the formation of **4** and **5**, complex **3** acts as tri- and didentate metalloligands through both its S and N atoms to connect the Cu atoms, leading to 2D and 3D frameworks. This work demonstrates wider possibilities for the construction of new heterometallic thiolate coordination polymers containing both main-group elements and transition metals under solvothermal conditions. Further efforts to expand this work by using other appropriate Sb sources, such as $[Sb_2(edt)_2S]$ and $[Sb_2(edt)_2S_2]$ are underway.

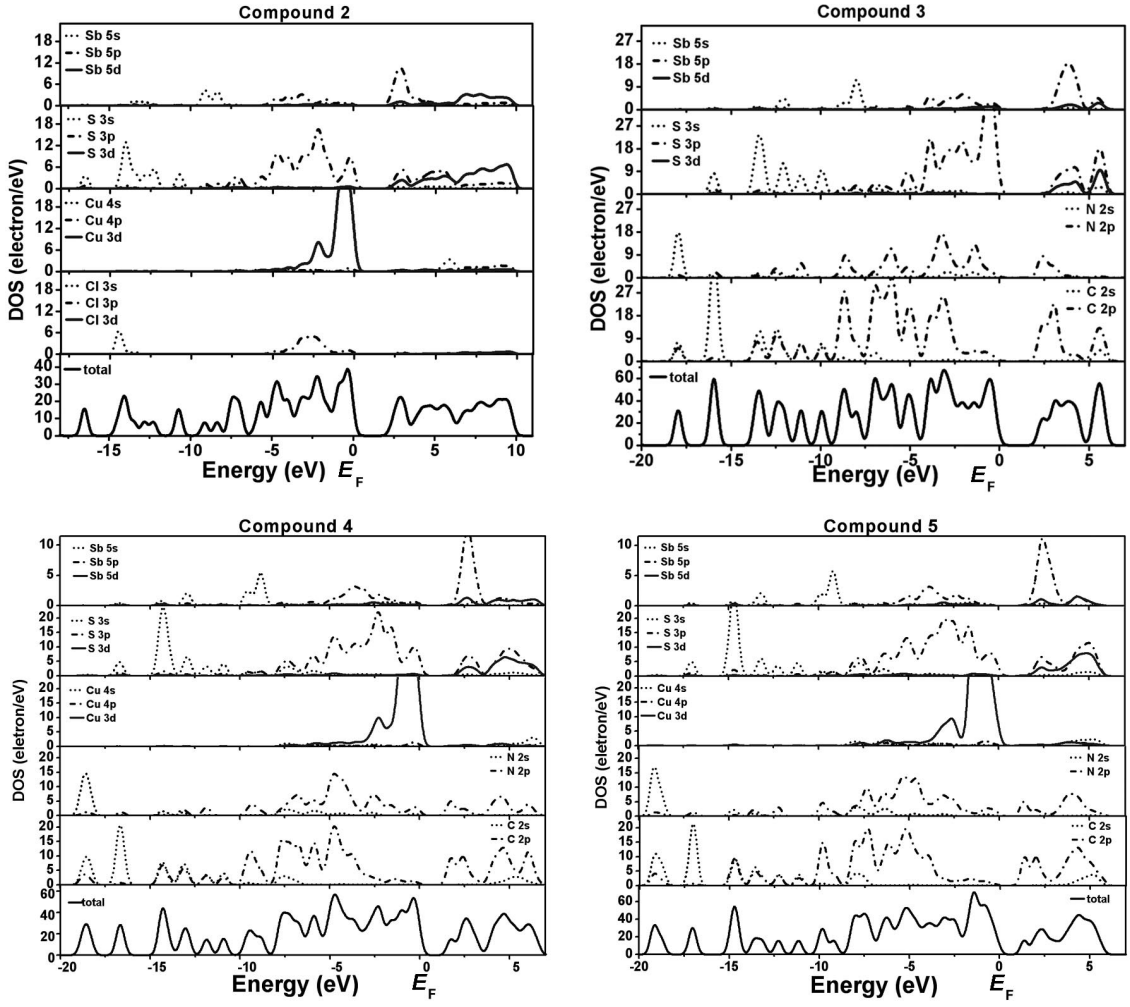

Figure 6. DOS plots of compounds **2**–**5** with the Fermi level set as zero.

Experimental Section

Material and Methods: Compound **1** was prepared according to literature procedures.[11] CuSCN, pymtH, $SbCl_3$, and H_2edt were all analytical reagents and used without further purification. CH_3CN, EtOH, and acetone were purified by standard methods before use. All the solvothermal reactions were carried out in glass tubes ($15.0 \times 0.8 \times 0.8$ cm^3). Infrared spectra were recorded with a Nicolet Magna 750 FT-IR spectrophotometer (KBr pellets). Elemental analyses were carried out using a Perkin–Elmer 2400 II elemental analyzer. The diffuse reflectance spectrum was measured with a Lambda 900 spectrophotometer using $BaSO_4$ powder for the 100% reflectance reference at room temperature. Power X-ray diffraction (XRD) patterns were recorded by BDX300 X-ray diffraction with Cu-K_α radiation (λ = 0.154 nm). ^{1}H and ^{13}C NMR spectroscopy was recorded with a Varian UNITY-500 spectrometer at room temperature; chemical shifts are quoted on the δ scale (downfield shifts are positive) relative to tetramethylsilane.

Calculation Methods and Details: DFT calculations were performed by using the periodic code of DMOL3 from Accelrys.[23a] The general gradient approximation[23b] plus Hamprecht–Cohen–Tozer–Handy approximation[23c] (GGA-HCTH) and the DNP basis set, which is comparable to the Gaussian 6-31G**, were used in all calculations. The global real space cutoff radius was 4.7 Å. The density-functional semicore pseudopotentials (DSPP)[23d] were used for all elements. In this scheme, all electrons for H, C, N, S, and Cl are included, whereas for Cu and Sb the $3s^23p^63d^{10}4s^1$ and $4d^{10}5s^25p^3$ electrons were treated as valence electrons, respectively. Accurate Brillouin zone sampling was chosen according to the Monkhorst–Pack[23e] scheme with a grid spacing of 0.04 $Å^{-1}$. A Fermi smearing of 0.005 hartree was employed to improve computational performance. The self-consistent-field procedures were performed with a convergence criterion of 10^{-6} a.u. on the total energy and electron density.

Crystal Structure Analyses: Suitable single crystals of the compounds were carefully selected and glued to thin glass fibers with epoxy resin. Intensity data were collected at room temperature with a Rigaku Mercury CCD area-detector diffractometer with a graphite monochromator utilizing Mo-K_α radiation (λ = 0.71073 Å). The structures were solved by direct methods and refined on F^2 by full-matrix least-squares analysis using the SHELXL-97 program package.[24] All non-hydrogen atoms were refined anisotropically. The positions of all hydrogen atoms in edt and pymt ligands were generated geometrically (C–H 0.97 or 0.93 Å), and U(H) values were set as 1.2 times U_{eq}(C). In compound **3**, the unique C atom connected to S1 is disordered over two positions, and was refined as two atoms of half occupancy, namely, C1 and C1′. The Flack parameter of compound **5** was 0.06(2). The crystallographic data for **2**–**5** are listed in Table 1. Selected bond lengths and angles for **2**–**5** are given in Table S1.

Table 1. Crystallographic data for complexes **2**–**5**.

	2	**3**	**4**	**5**
Empirical formula	$C_5H_8ClCu_2NS_6Sb_2$	$C_6H_7N_2S_3Sb$	$C_{15}H_{14}Cu_3N_7S_9Sb_2$	$C_8H_7Cu_2N_4S_5Sb$
Fw	680.51	325.07	1014.99	568.31
Crystal system	orthorhombic	monoclinic	triclinic	orthorhombic
Space group	*Pmc*2(1)	*C*2/*c*	$P\bar{1}$	*Iba*2
a (Å)	10.715(5)	20.782(9)	6.962(2)	43.256(3)
b (Å)	6.095(3)	8.573(3)	13.757(3)	6.9566(5)
c (Å)	11.474(5)	15.52(1)	15.871(4)	10.6961(7)
α (°)	90.00	90.00	108.171(3)	90.00
β (°)	90.00	131.139(5)	92.343(2)	90.00
γ (°)	90.00	90.00	98.838(2)	90.00
V (Å^3)	749.4(6)	2083(2)	1420.7(6)	3218.6(4)
Z	2	8	2	8
D_{calcd} (g cm^{-3})	3.016	2.073	2.373	2.346
μ (mm^{-1})	7.353	3.199	4.770	4.925
$F_{(ooo)}$	636	1248	972	2176
Parameters	89	109	325	182
R_1[a], wR_2[b] [$I > 2\sigma(I)$]	0.0228/0.0413	0.0219/0.0613	0.0210/0.0459	0.0363/0.0546
R_1[a], wR_2[b] [all data]	0.0270/0.0424	0.0251/0.0624	0.0283/0.0482	0.0446/0.0577
Goodness-of-fit on F^2	0.998	1.082	0.977	1.056

[a] $R_1 = \Sigma||F_o|-|F_c||/\Sigma|F_o|$. [b] $wR_2 = [\Sigma w(F_o^2 - F_c^2)^2/\Sigma w(F_o^2)^2]^{0.5}$.

CCDC-649556 (**2**), 649557 (**3**), 649558 (**4**), and 658415 (**5**) contain the supplementary crystallographic data for this paper. These data can be obtained free of charge from the Cambridge Crystallographic Data Centre via www.ccdc.cam.ac.uk/data_request/cif.

Synthesis of [{Sb$_2$(edt)$_2$SCuCl(CuSCN)}$_n$] (2): Compound **1** (50 mg, 0.2 mmol), CuSCN (24 mg, 0.2 mmol), and acetone (2.0 mL) were placed in a glass tube. The tube was evacuated and sealed before it was heated at 120 °C for 48 h. After cooling the tube to room temperature over 40 h, pale yellow crystals suitable for X-ray single-crystal diffraction were formed. Yield 10 mg (14% based on Sb). $C_5H_8ClCu_2NS_6Sb_2$ (680.51): calcd. C 8.82, H 1.18, N 2.06; found C 8.94, H 1.21, N 2.01. IR (KBr pellet): $\tilde{\nu}$ = 2078 (s), 1385 (s), 1234 (w), 1122 (m), 917 (w), 831 (m), 669 (m), 636 (w), 418 (w) cm^{-1}.

Synthesis of [Sb(edt)(pymt)] (3): Compound **3** was synthesized by standard Schlenk techniques under a purified nitrogen atmosphere. To a solution of compound **1** (0.98 g, 4.0 mmol) in EtOH (20 mL) was added a solution of pymtNa (4.0 mmol; prepared in situ by treating sodium with pymtH in EtOH) at 50 °C. The mixture was heated at reflux for 4 h, cooled to room temperature, and white solid (0.82 g, 63% yield) was collected by filtration and washed with H_2O, EtOH, and Et_2O. White crystals suitable for X-ray single-crystal diffraction could be obtained by crystallization of **3** from EtOH or acetone. $C_6H_7N_2S_3Sb$ (325.07): calcd. C 22.17, H 2.17, N 8.62; found C 21.98, H 2.49, N 8.40. IR (KBr pellet): $\tilde{\nu}$ = 1557 (m), 1541 (m), 1371 (s), 1173 (m), 834 (w), 808 (w), 767 (w), 743 (m), 637 (w) cm^{-1}. ^{1}H NMR ($CDCl_3$): δ = 3.62–3.65 (s, 4 H, -CH_2–S-), 7.03–7.06 (w, 1 H, C=CH-C), 8.45–8.46 (m, 2 H, N=CH–C) ppm. ^{13}C NMR ($CDCl_3$): δ = 41.00–41.52 (s, 2 C, -CH_2–S-), 116.37–116.71 (w, 1 C, the middle C of C–CH=C in pymt), 156.67–156.87 (m, 2 C, N=CH-), 174.28 (w, 1 C, S–C=N) ppm.

Synthesis of [{[Sb(edt)(pymt)]$_2$(CuSCN)$_3$}$_n$] (4): The synthesis of **4** is similar to that of **2**. Compound **3** (33 mg, 0.1 mmol), CuSCN (18 mg, 0.15 mmol), and CH_3CN (2.0 mL) were placed in a glass tube and heated at 120 °C for 48 h. Yellow block crystals formed upon cooling to room temperature over 32 h. Yield 37 mg (73% based on Sb). $C_{15}H_{14}Cu_3N_7S_9Sb_2$ (1014.99): calcd. C 17.75, H 1.39, N 9.66; found C 17.94, H 1.31, N 9.83. IR (KBr pellet): $\tilde{\nu}$ = 2100 (s), 1558 (w), 1547 (m), 1375 (s), 1183 (m), 844 (w), 810 (w), 760 (w), 748 (m), 649 (w) cm^{-1}.

Synthesis of [{[Sb(edt)(pymt)](CuSCN)$_2$}$_n$] (5): The synthesis of **5** is same as that of **4** except that the quantity of CuSCN used was 24 mg (0.2 mmol). Some yellow block crystals of **4** were formed in the bottom of the tube and orange-red crystals of **5** were formed on the tube wall. Compound **5** could be collected carefully by using a microscope. Yield 9 mg (16% based on Sb). $C_8H_7Cu_2N_4S_5Sb$ (568.31): calcd. C 16.91, H 1.24, N 9.86; found C 16.78, H 1.32, N 10.02. IR (KBr pellet): $\tilde{\nu}$ = 2126 (s), 1554 (m), 1541 (m), 1371 (s), 1174 (m), 800 (w), 757 (w), 744 (w) cm^{-1}.

Supporting Information (see footnote on the first page of this article): Selected bonds lengths and angles of compounds **2**–**5**, XPRD patterns of **3**, packing diagrams of compounds **2** and **4**, plots of $(a/s)^2$ vs. photon energy for compounds **1**–**5** and CuSCN.

Acknowledgments

This work was supported by grants from the State Key Laboratory of Structural Chemistry, Fujian Institute of Research on the Structure of Matter, Chinese Academy of Sciences (CAS), (SZD08002–2), National Basic Research Program of China (973 Program, 2007CB815306), the National Natural Science Foundation of China (20733003 and 20673117), and Knowledge Innovation Program of the Chinese Academy of Sciences.

[1] a) W. H. Armstrong, R. H. Holm, *J. Am. Chem. Soc.* **1981**, *103*, 6246–6248; b) T. E. Wolff, J. M. Bergm, P. P. Power, K. O. Hodgson, R. H. Holm, *Inorg. Chem.* **1980**, *19*, 430–437; c) D. Sellmann, F. Lauderbach, F. Geipel, F. W. Heinemann, M. Moll, *Angew. Chem. Int. Ed.* **2004**, *43*, 3141–3144; d) C. N. Chen, T. B. Wen, W. J. Li, H. P. Zhu, Y. H. Chen, Q. T. Liu, J. X. Lu, *Inorg. Chem.* **1999**, *38*, 2375–2379.

[2] a) D. Fenske, M. Bettenhausen, *Angew. Chem. Int. Ed.* **1998**, *37*, 1291–1294; b) X. Wang, T. L. Sheng, R. B. Fu, S. M. Hu, S. C. Xiang, L. S. Wang, X. T. Wu, *Inorg. Chem.* **2006**, *45*, 5236–5238; c) R. Ahlrichs, A. Eichhöfer, D. Fenske, K. May, H. Sommer, *Angew. Chem. Int. Ed.* **2007**, *46*, 8254–8257.

[3] a) W. Hirpo, S. Dhingra, A. C. Sutorik, M. G. Kanatzidis, *J. Am. Chem. Soc.* **1993**, *115*, 1597–1599; b) C. Krebs, T. Glaser, E. Bill, T. Weyhermüller, W. Meyer-Klancke, K. Wieghardt, *Angew. Chem. Int. Ed.* **1999**, *38*, 359–361; c) J. L. Xie, X. H. Bu, N. F. Zheng, P. Y. Feng, *Chem. Commun.* **2005**, 4916–4918;

d) K. K. Banger, M. H. C. Jin, J. D. Harris, P. E. Fanwick, A. F. Hepp, *Inorg. Chem.* **2003**, *42*, 7713–7715.

[4] For examples, see: a) R. Panda, C. P. Berlinguette, Y. Zhang, R. H. Holm, *J. Am. Chem. Soc.* **2005**, *127*, 11092–11101; b) Q. C. Zhang, X. H. Bu, J. Zhang, T. Wu, P. Y. Feng, *J. Am. Chem. Soc.* **2007**, *129*, 8412–8413; c) Z. H. Li, S. W. Du, X. T. Wu, *Inorg. Chem.* **2004**, *43*, 4776–4777.

[5] a) S. S. Garje, V. K. Jain, *Coord. Chem. Rev.* **2003**, *236*, 35–56; b) C. Silvestru, I. Haiduc, *Coord. Chem. Rev.* **1996**, *147*, 117–146; c) R. C. Mehotra, G. Srivastava, B. P. S. Chauhan, *Coord. Chem. Rev.* **1984**, *55*, 207–259; d) M. A. Pitt, D. W. Johnson, *Chem. Soc. Rev.* **2007**, *36*, 1441–1453.

[6] a) N. Avarvari, E. Faulques, M. Fourmigué, *Organometallics* **2003**, *22*, 2042–2049; b) N. Avarvari, E. Faulques, M. Fourmigué, *Inorg. Chem.* **2001**, *40*, 2570–2577; c) N. Avarvari, M. Fourmigué, E. Canadell, *Eur. J. Inorg. Chem.* **2004**, 3409–3414.

[7] a) I. I. Ozturk, S. K. Hadjikakou, N. Hadjiliadis, N. Kourkoumelis, M. Kubicki, M. Baril, I. S. Butler, J. Balzarini, *Inorg. Chem.* **2007**, *46*, 8652–8661; b) S. K. Hadjikakou, C. D. Antoniadis, N. Hadjiliadis, M. Kubicki, J. Binolis, S. Karkabounas, K. Charalabopoulos, *Inorg. Chim. Acta* **2005**, *358*, 2861–2866; c) S. M. S. V. Doidge-Harrison, J. T. S. Irvine, G. M. Spencer, J. L. Wardell, M. Wei, P. Ganis, G. Valle, *Inorg. Chem.* **1995**, *34*, 4581–4584; d) E. Block, G. Ofori-Okai, H. Kang, J. Wu, J. Zubieta, *Inorg. Chem.* **1991**, *30*, 4784–4788; e) M. Peters, W. Saak, S. Pohl, *Z. Anorg. Allg. Chem.* **1996**, *622*, 2119–2123.

[8] a) T. Matsumoto, Y. Matsui, M. Ito, K. Tatsumi, *Inorg. Chem.* **2008**, *47*, 1901–1903; b) L. T. Abrantes, N. M. Comerlato, G. B. Ferreira, R. A. Howie, J. L. Wardell, *Inorg. Chem. Commun.* **2006**, *9*, 522–525; c) H. P. S. Chauhan, U. P. Singh, N. M. Shaik, S. Mathur, V. Huch, *Polyhedron* **2006**, *25*, 2841–2847.

[9] a) J. G. Alvarado-Rodríguez, N. Andrade-López, S. González-Montiel, M. Merino, A. Vela, *Eur. J. Inorg. Chem.* **2003**, 3554–3562; b) J. G. Alvarado-Rodríguez, S. González-Montiel, N. Andrade-López, L. B. López-Feliciano, *Polyhedron* **2007**, *26*, 2929–2934.

[10] a) A. J. Barton, N. J. Hill, W. Levason, B. Patel, G. Reid, *Chem. Commun.* **2001**, 95–96; b) A. J. Barton, N. J. Hill, W. Levason, G. Reid, *J. Chem. Soc., Dalton Trans.* **2001**, 1621–1627.

[11] a) G. Bandoli, A. Dolmella, V. Peruzzo, G. Plazzogna, *Inorg. Chim. Acta* **1993**, *204*, 153–157; b) M. A. Bush, P. F. Lindley, P. Woodward, *J. Chem. Soc. A* **1967**, 221–227; c) P. E. Garrou, G. E. Hartwell, *Inorg. Chem.* **1976**, *15*, 730–732; d) M. A. Arif, D. J. Chandler, R. A. Jones, *J. Coord. Chem.* **1987**, *16*, 213–218; e) L. W. Clemence, M. T. Leffler, *J. Am. Chem. Soc.* **1948**, *70*, 2439–2440.

[12] a) H. O. Stephan, M. G. Kanatzidis, *J. Am. Chem. Soc.* **1996**, *118*, 12226–12227; b) N. Ding, M. G. Kanatzidis, *Chem. Mater.* **2007**, *19*, 3867–3869; c) M. Zhang, T. L. Sheng, X. H. Huang, R. B. Fu, X. Wang, S. M. Hu, S. C. Xiang, X. T. Wu, *Eur. J. Inorg. Chem.* **2007**, 1606–1612; d) R. Stähler, W. Bensch, *J. Chem. Soc., Dalton Trans.* **2001**, 2518–2522; e) M. Schaefer, R. Stähler, W. R. Kiebach, C. Näther, W. Bensch, *Z. Anorg. Allg. Chem.* **2004**, *630*, 1816–1822; f) P. Vaqueiro, A. M. Chippindale, A. V. Powell, *Inorg. Chem.* **2004**, *43*, 7963–7965; g) Y. Matsushita, Y. Ueda, *Inorg. Chem.* **2003**, *42*, 7830–7838; h) P. Vaqueiro, A. M. Chippindale, A. V. Powell, *Polyhedron* **2003**, *22*, 2839–2845.

[13] a) P. Vaqueiro, A. M. Chippindale, A. R. Cowley, A. V. Powell, *Inorg. Chem.* **2003**, *42*, 7846–7851; b) P. T. Wood, G. L. Schimek, J. W. Kolis, *Chem. Mater.* **1996**, *8*, 721–726; c) A. V. Powell, J. Thun, A. M. Chippindale, *J. Solid State Chem.* **2005**, *178*, 3414–3419.

[14] a) V. Spetzler, C. Näther, W. Bensch, *Inorg. Chem.* **2005**, *44*, 5805–5812; b) A. V. Powell, R. Paniagua, P. Vaqueiro, A. M. Chippindale, *Chem. Mater.* **2002**, *14*, 1220–1224; c) G. L. Schimek, J. W. Kolis, G. J. Long, *Chem. Mater.* **1997**, *9*, 2776–2785; d) A. V. Powell, S. Boissière, A. M. Chippindale, *J. Chem. Soc., Dalton Trans.* **2000**, 4192–4195; e) V. Spetzler, H. Rijnberk, C. Näther, W. Bensch, *Z. Anorg. Allg. Chem.* **2004**, *630*, 142–148; f) C. Wang, R. C. Haushalter, *Inorg. Chim. Acta* **1999**, *288*, 1–6.

[15] X. P. Zhou, D. Li, T. Wu, X. J. Zhang, *Dalton Trans.* **2006**, 2435–2443.

[16] A. Lipka, *Z. Anorg. Allg. Chem.* **1980**, *466*, 195–202.

[17] Z. M. Hao, X. M. Zhang, *Cryst. Growth Design.* **2007**, *7*, 64–68.

[18] a) N. Burford, T. M. Parks, B. W. Royan, B. Boreck, T. S. Cameron, J. F. Richardson, E. J. Gabe, R. Hynes, *J. Am. Chem. Soc.* **1992**, *114*, 8147–8151; b) T. A. Shaikh, R. C. Bakus II, S. Parkin, D. A. Atwood, *J. Organomet. Chem.* **2006**, *691*, 1825–1833.

[19] a) L. J. Bellamy, *The Infrared Spectra of Complex Molecules*, Wiley, New York, **1966**; b) T. S. Lobana, R. Sharma, G. Hundal, R. J. Butcher, *Inorg. Chem.* **2006**, *45*, 9402–9409; c) L. Han, M. C. Hong, R. H. Wang, B. L. Wu, Y. Xu, B. Y. Lou, Z. Z. Lin, *Chem. Commun.* **2004**, 2578–2579; d) D. Li, W. J. Shi, L. Hou, *Inorg. Chem.* **2005**, *44*, 3907–3913.

[20] a) G. Kotüm, *Reflectance Spectroscopy*, Springer-Verlag, New York, **1969**; b) W. W. Wendlandt, H. G. Hecht, *Reflectance Spectroscopy*, Interscience Publishers, New York, **1966**.

[21] G. Cao, L. K. Rabenberg, C. M. Nunn, T. E. Mallouk, *Chem. Mater.* **1991**, *3*, 149–156.

[22] a) H. J. Tromp, P. Gelderen, P. J. Kelly, G. Brocks, P. A. Bobbert, *Phys. Rev. Lett.* **2001**, *87*, 016401, 1–4; b) L. J. Sham, M. Schlüter, *Phys. Rev. Lett.* **1983**, *51*, 1888–1891; c) J. P. Perdew, M. Levy, *Phys. Rev. Lett.* **1983**, *51*, 1884–1887.

[23] a) B. Delley, *J. Chem. Phys.* **2000**, *113*, 7756–7764; b) J. P. Perdew, K. Burke, M. Ernzerhof, *Phys. Rev. Lett.* **1996**, *77*, 3865–3868; c) A. D. Boese, C. H. Nicholas, *J. Chem. Phys.* **2001**, *114*, 5497–5503; d) B. Delley, *Phys. Rev. B* **2002**, *66*, 155125, 1–6; e) H. J. Monkhorst, J. D. Pack, *Phys. Rev. B* **1976**, *13*, 5188–5192.

[24] a) G. M. Sheldrick, *SHELXS-97 Program for X-ray Crystal Structure Solution*, University of Göttingen, Germany, **1997**; b) G. M. Sheldrick, *SHELXL-97 Program for X-ray Crystal Structure Refinement*, University of Göttingen, Germany, **1997**.

Received: October 21, 2008
Published Online: January 8, 2009

